Geophysical Journal International

Geophys. J. Int. (2012) **191,** 1205–1209 doi: 10.1111/j.1365-246X.2012.05700.x

EXPRESS LETTER

Virtual electrode current injection using seismic focusing and seismoelectric conversion

Paul Sava[1] and André Revil[1,2]

[1] *Colorado School of Mines, Department of Geophysics, Golden,* 80401, *CO, USA. E-mail: psava@mines.edu (PS), arevil@mines.edu (AR)*
[2] *ISTerre, CNRS, UMR CNRS* 5275, *Université de Savoie,* 73376 *cedex, Le Bourget du Lac, France*

Accepted 2012 September 26. Received 2012 September 1; in original form 2012 July 4

SUMMARY

Acoustic wavefields produced using sources appropriately delayed in time can be focused at known positions and times in a heterogeneous medium. Seismoelectric conversion occurs if the acoustic focus point coincides with a discontinuity in electrical and hydrological medium properties, thus generating a current density. The current generates a potential difference, which can be observed at a distance by an array of monitoring electrodes. Since the acoustic wavefield is precisely located at a position and time, this electrical source behaves like a controlled virtual electrode whose properties depend on the strength of the acoustic wavefield and on the medium properties. This procedure can be used to increase the robustness and resolutions of electrical resistivity tomography and to identify hydrological parameters at various points in the medium by scanning the medium by changing the position of the acoustic focus point.

Key words: Interferometry; Electrical properties; Wave propagation; Acoustic properties.

INTRODUCTION

Electrical resistivity tomography derives from the seminal works of Wenner (1912, 1915) and Schlumberger (1920). The classical way to do electrical resistivity tomography is to inject/retrieve an electrical current into the ground and measure a difference of electrical potential at a set of potential electrodes. The main drawback of this methodology is that the sensitivity is mainly localized in the vicinity of the electrodes, thus limiting the ability of this geophysical method to image a wide area with high resolution (Haines 2004).

We propose a new approach designed to add additional information to electrical resistivity tomography by emulating virtual current injection at any point of space thorough focusing of seismic energy and electrical current generated by electrokinetic conversion. We exploit the fact that seismic waves propagating in an elastic medium trigger a volumetric current density at places of discontinuity in electrical (e.g. conductivity) and hydraulic properties (e.g. permeability). The seismoelectric theory describes the coupling between seismic wave propagation and the generation of electromagnetic disturbances of electrokinetic nature (Frenkel 1944). The transfer function characterizing this phenomenon represents an extension of the well-known electrokinetic theory in porous media and capillaries (Helmholtz 1879). The seismoelectric conversion happens everywhere in the medium, but its largest intensity occurs at locations characterized by the highest gradient of material properties. The volumetric current density, in turn, generates an electrical field through an electrokinetic coupling mechanisms and this electrical field can be remotely observed using an array of electrodes distributed in the medium.

This electrical field can be used to invert the resistivity distribution through electrical resistivity tomography, and the seismoelectric conversion, that is, the volumetric current density, can be used to characterize the petrophysical (mechanical, hydraulic and electrical) properties of the area where the seismic source focus. Usually only a small number of elastic sources and electrodes are employed for a seismoelectric survey, which limits our ability to characterize the medium with high resolution. The strength of the seismoelectric source depends on the intensity of the elastic field, which is variable in space and time, and the strength of the observed electric potential depends on the conductivity of the medium, which is heterogeneous as a function of space. It is, therefore, difficult to unambiguously characterize the electric properties of the medium throughout the space under investigation, especially at the source, because the seismic wavefield spreads throughout the medium and low intensity electric signals are triggered everywhere in the medium.

We advocate a different seismoelectric procedure, based on controlled sources as a function of space and time. We propose that a synchronized array of seismic sources with different, but known, source functions be used instead of individual point sources. These sources can be appropriately phase delayed such that waves propagating through the medium accumulate (i.e. focus) at known locations and at known times. At the focus time, seismoelectric conversion occurs mostly at the known focus location and with much larger strength compared with that of the seismoelectric

conversion occurring throughout the medium both before and after focusing occurs. In this way, we can construct 'virtual electrodes' which inject energy into the medium at known times and locations, thus reducing the ambiguity posed by seismoelectric analysis in a heterogeneous medium. We can control not only the position and time of the sources, but also their strength and time evolution.

We assume in our technique that the elastic properties of the medium are known with sufficient accuracy, for example, from wavefield tomography (Tarantola 1984, 1987; Pratt & Worthington 1990; Woodward 1992; Plessix 2006), such that the elastic wavefield can be reliably focused at a known location and at a known time. As discussed in more detail in the following sections, the strength of the observed seismoelectric potential depends on the acoustic field, but also on the (unknown) petrophysical properties at the source including the (unknown) electric properties in the medium. Identifying these properties is our main goal, and this can be accomplished through conventional seismoelectric inversion. That said, here we do not discuss about electrical resistivity tomography, but we focus on the forward problem and discuss how controlled virtual electrodes can aid seismoelectric inversion. We also assume, for simplicity, that we operate in the quasi-static regime of the Maxwell equations [see Hu & Liu (2002); Hu *et al.* (2007); Jardani *et al.* (2010) for a justification of this assumption], although this is not a fundamental limitation of our technique.

THEORY

The seismoelectric problem is usually formulated in terms of a coupling between the Maxwell equations and the Biot theory (Pride 1994; Haines 2004; Revil & Jardani 2010). For simplicity, we adapt the seismoelectric theory to make it compatible with the acoustic approximation, although our methodology is not limited to seismoelectric effects caused by acoustic wavefields.

In the acoustic approximation, we solve for the pressure P, which corresponds to the hydrostatic component of the macroscopic stress tensor $\overline{\overline{\mathbf{T}}}$,

$$P = -\frac{1}{3}\mathtt{tr}\,(\overline{\overline{\mathbf{T}}}), \tag{1}$$

where $\mathtt{tr}\,(\overline{\overline{\mathbf{T}}})$ represents the trace of the stress tensor. We can evaluate the pressure P directly by solving an acoustic wave equation, for example,

$$\frac{\partial^2 P}{\partial t^2} - K\nabla\cdot\left(\frac{1}{\rho}\nabla P\right) = f(\mathbf{x},t), \tag{2}$$

where $\mathbf{x}$ and t denote space and time, respectively, K and ρ are the rock bulk modulus and density, respectively, and f represents the acoustic source. This formulation allows us to simulate a pressure field using an arbitrary source distribution as a function of space and time. For example, a typical band-limited point source at coordinates $\mathbf{x}_0$ can be represented by

$$f(\mathbf{x},t) = \delta(\mathbf{x}-\mathbf{x}_0)\,w(t), \tag{3}$$

where $w(t)$ is a wavelet confined to a certain frequency band. However, focusing at a given point in the medium $\mathbf{x}_\mathrm{s}$ from a distributed receiver array at coordinates $\mathbf{x}_\mathrm{r}$ can be achieved using time reversal with appropriately delayed sources injected at all receivers. An easy procedure to obtain the source delays is to simulate the acoustic wavefield forward in time with a source at $\mathbf{x}_\mathrm{s}$ and observations at the receivers located at coordinates $\mathbf{x}_\mathrm{r}$, although this is not the only possibility. This process is akin of time-reversal employed in, for example, non-destructive testing (Prada *et al.* 2002), ocean acoustics (Parvulescu & Clay 1965), seismic imaging (Clærbout 1985), medical imaging (Fink 1997; Fink & Prada 2001) and earthquake seismology (Rietbrock & Scherbaum 1994).

For the seismoelectric problem, we need to relate the pressure applied on the material to a change in the pore fluid pressure. In the undrained regime of poroelasticity, the pressure P is related to the so-called undrained pore fluid pressure p by

$$p = BP, \tag{4}$$

where the Skempton coefficient $0 \leq B \leq 1$ is given by

$$B = \frac{1 - K/K_\mathrm{u}}{1 - K/K_\mathrm{s}}, \tag{5}$$

where K is the bulk modulus, K_u is the undrained bulk modulus and K_s the bulk modulus of the solid phase. The passage of the acoustic wave generates pressure fluctuations, which in turn change the pore fluid pressure and therefore lead to flow of the pore water according to Darcy's law:

$$\mathbf{u} = -\frac{k}{\eta_\mathrm{w}}\nabla p\ . \tag{6}$$

In this equation, $\mathbf{u}$ denotes the Darcy velocity (macroscopic volumetric flux of water), k is the permeability and η_w is the pore water dynamic viscosity (typically 10^{-3} Pa s). The excess charge in the pore water, which counterbalances the deficiency of charge of the mineral surface, is dragged by the pressure-induced flow of water, thus generating an electrical current density. The source current density associated with the pore water flow induced by the seismic wave is Jardani *et al.* (2010)

$$\mathbf{j}_s = \hat{Q}_V\mathbf{u}\ . \tag{7}$$

If we substitute the expression of the Darcy velocity we obtain

$$\mathbf{j}_s = -\hat{Q}_V\frac{k}{\eta_\mathrm{w}}\nabla p, \tag{8}$$

where the quantity $\hat{Q}_V$ denotes the excess of charges contained in the pore water. To reduce the number of unknowns, the volumetric charge density can be obtained from the permeability itself using the empirical relationship $\log_{10}(\hat{Q}_V) = -9.23 - 0.82\log_{10}(k)$ (Jardani *et al.* 2007; Revil & Jardani 2010). This charge density is due to the electrical diffuse layer coating the surface of the grains (Wang & Revil 2010).

The total current density $\mathbf{j}$ is the sum of a conduction current density plus the source current density associated with the flow of the pore water $\mathbf{j}_s$ (Pride 1994; Jardani *et al.* 2007):

$$\mathbf{j} = \sigma\mathbf{E} + \mathbf{j}_s, \tag{9}$$

where $\mathbf{E} = -\nabla\psi$ is the quasi-static electrical field, and σ denotes the electrical conductivity of the porous rock. The quasi-static regime is a good approximation if the distance between the source and the receivers is typically smaller than 1 km (Jardani *et al.* 2010; Araji *et al.* 2012). The quasi-static continuity equation, which corresponds to the charge conservation equation, is

$$\nabla\cdot\mathbf{j} = 0. \tag{10}$$

The volumetric source current density, caused by the passage of a wave through a heterogeneous material, is responsible for the radiation of electromagnetic energy. Therefore, under the quasi-static limit of the Maxwell equations, the electrical potential ψ is governed by the Poisson equation:

$$\nabla\cdot(\sigma\nabla\psi) = \nabla\cdot\mathbf{j}_s\ . \tag{11}$$

This equation represents the partial differential equation we need to solve to evaluate the electric potential ψ given by an electroacoustic source current $\mathbf{j}_s$. The right-hand side represents a source term for the electrostatic problem:

$$\nabla \cdot \mathbf{j}_s = \nabla \cdot \left[\hat{Q}_V \frac{k}{\eta_w} \nabla (BP) \right], \tag{12}$$

where the pressure P is obtained by solving an acoustic wave equation, for example, eq. (2). This relation shows explicitly how the heterogeneities in k and B generate radiative electrical fields that can be instantaneously measured at all the electrodes deployed in the medium.

In summary, seismoelectric virtual electrodes can be constructed at a given position in the medium by simulating an acoustic wavefield, which focuses at the desired coordinates (eq. 2). The pressure change at the focus point induces in the medium a current (eq. 8), from which we can construct an electric source (eq. 12), and solve for the quasi-static electrical potential $\psi(\mathbf{x})$ in the entire domain of investigation. As indicated earlier, this electrical source occurs at a known time and position and it has the largest amplitude relative to all other propagation times. The wavefield spatial and temporal localization enables us to describe the electrical source as a controlled virtual electrode.

EXAMPLES

We illustrate our methodology with two synthetic examples. In both cases, we use typical material properties characterizing a porous and permeable material (e.g. water-saturated sand) and an impermeable material (e.g. water-saturated shale):

Parameter	Unit	Reservoir	Non-Reservoir
Bulk modulus	Pa	22×10^9	7×10^9
Density	$\mathrm{kg\,m^{-3}}$	2300	1900
Conductivity	$\mathrm{S\,m^{-1}}$	0.01	1.00
Skempton coefficient		0.65	0.85
Permeability	$\mathrm{m^2}$	10^{-12}	10^{-16}

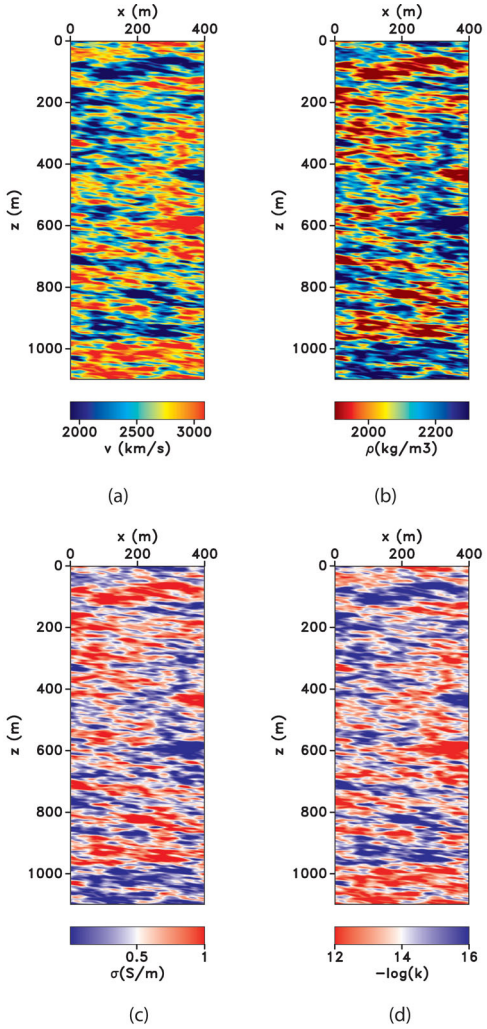

Figure 1. Physical parameters characterizing a heterogeneous model: (a) velocity, (b) density, (c) conductivity and (d) permeability.

For both examples, we assume that two borehole seismic arrays are deployed in the medium. The borehole arrays are sufficiently wide to facilitate energy focusing at various locations in the medium and at different times. We assume that the boreholes are relatively shallow, such that we can treat the surface as an insulating boundary. All other boundaries are conductive, thus simulating and unbounded volume.

The first example represents a heterogeneous earth model characterized by the velocity, density, conductivity and permeability depicted in Figs 1(a)–(d). In this numerical experiment, we simulate a virtual seismoelectric electrode at location $\{x, z\} = \{200, 650\}$ m. Using the 525 acoustic receivers located in each of the boreholes located at $x = 50$ m and $x = 350$ m, we backpropagate acoustic waves phased appropriately to focus at the target point at a known time, arbitrarily chosen as $t = 0$ s.

The left panels in Figs 2(a)–(d) show the wavefields focusing towards the virtual electrode location. The right panels of the same figures show the electric potential as a function of space at the respective time. We can observe that seismoelectric conversions occur throughout the medium, but with relatively low intensity corresponding to the distribution of the acoustic field. At the focus time, Fig. 2(d), the electric potential is strongest relative to all other times. This change of potential can then be observed at the electrodes, as depicted in the right panels of Figs 2(a)–(d).

This example demonstrates that we can simulate virtual electrodes with strength, position and time of occurrence controlled via a remote seismic array. Furthermore, as seen in Fig. 3, the strength of the electric potential is significantly larger when the wavefield is focused at a single location, relative to the times when the wavefield is spread out in the medium.

The second numerical example illustrates a different feature of our methodology. Using a similar type of seismic array, we focus the acoustic energy at different locations in the medium, thus probing the existence of contrasts of hydroelectric properties facilitating seismoelectric conversions. Figs 4(a)–(d) show the acoustic field, spatially dependent electric potential and observed electric potential for different virtual electrodes in the medium. All panels correspond to the focusing time, which is responsible for the strongest electric potential. We can observe that the electric potential changes significantly with position, due to the different medium parameters at the virtual electrode position. This example demonstrates that we can control the position of the virtual electrodes and that the strength of the observed electric potential depends on the medium parameters at the virtual electrode position.

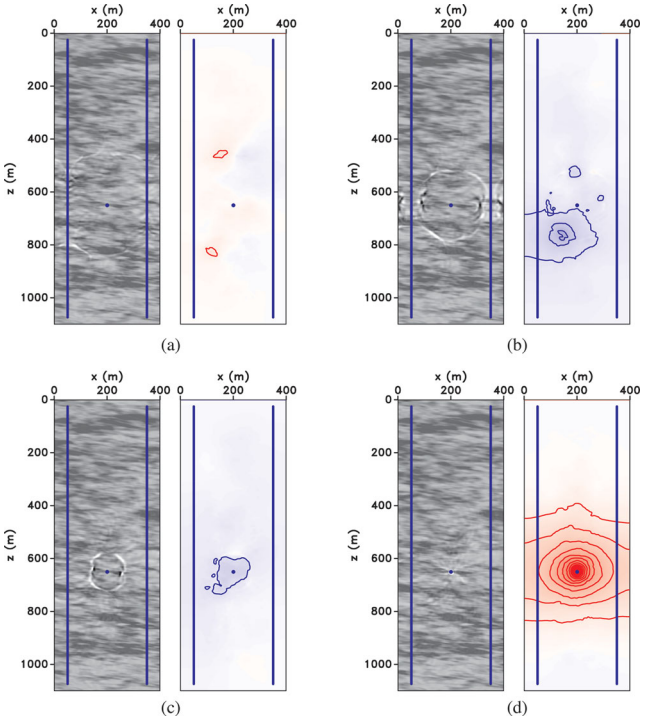

Figure 2. Acoustic wavefield (left panels) and electric potential (right panels) as a function of time. The figures correspond to various times during wavefield focusing at the virtual source.

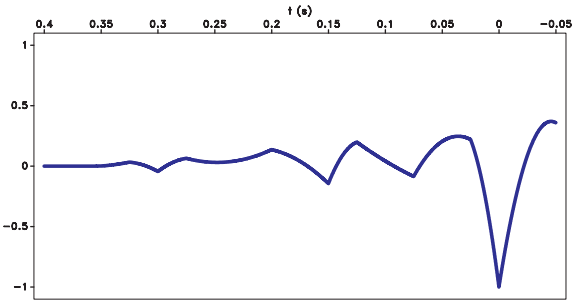

Figure 3. Normalized electric potential as a function of time at coordinates $\{x, z\} = \{50, 600\}$ m. The plot indicates the significantly stronger electric potential achieved when the wavefield is focused at a single location in the medium.

DISCUSSION

The methodology described in this paper can serve as the basis for electrical resistivity tomography with controlled virtual sources constructed at known locations and times. We can define different scenarios in which this methodology can be employed:

(1) Assuming that we know the conductivity in the medium, we can find the parameters of an electrical source at a known position and time. If the source is positioned at the interface between permeable and impermeable materials, then the inverted source can provide information about the permeability of the medium. This setup can be used to monitor fluid flow and fluid composition, as well.

(2) Assuming that we know the hydraulic properties at a certain location in the medium, we can find the electrical conductivity characterizing the space between the virtual electrode and the real electrodes located in nearby boreholes. In principle we can simulate

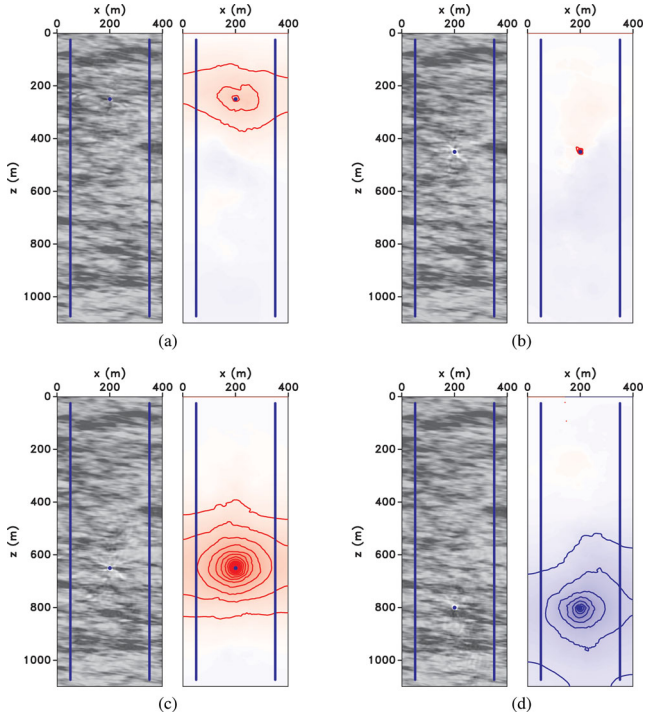

Figure 4. Acoustic wavefield (left panels) and electric potential (right panels) as a function of space. The figures correspond to various positions in the model characterized by different contrasts of physical properties.

an arbitrary number of virtual electrodes throughout the medium, thus increasing the resolution and robustness of electric tomography.

In general, however, those two problems are not separated and an inverse problem needs to incorporate both. One possibility to address this problem is by iterating between them to solve for the source and the medium. Moreover, we can cast the electrical resistivity tomography as a 4-D problem where we use the acoustic wavefield at all times as a time-variable source investigating the same model controlled by invariant parameters.

Finally we note that focusing of seismic energy could be simulated computationally through techniques like, for example, seismic interferometry (Thorbecke & Wapenaar 2007). This approach can also be used for interferometric Green's function representations of coupled electromagnetic and seismic wave propagation (De Ridder *et al.* 2009). Here we take a different approach and discuss about physical focusing achieved in a medium of known acoustic properties to evaluate the electric properties in its vicinity. Our approach, thus, provides direct access to seismoelectric sources excited in the medium.

CONCLUSIONS

We demonstrate that virtual electrodes can be simulated at known positions and times in a heterogeneous medium. This is achieved using focusing of acoustic waves at the specified coordinates from multiple acoustic receivers located in the vicinity of the target. The acoustic energy at the focus time is the largest relative to all other times, thus insuring the strongest possible seismoelectric source at the target position. This methodology can be used to investigate the electric and hydraulic properties of a medium by surrounding the area of investigation with multiple electrodes at known positions. The dense virtual electrode distribution has the potential to increase the robustness and to improve the resolution of electrical resistivity

tomography. This methodology can also be employed to infer hydraulic parameters, for example, permeability, through a controlled seismoelectric procedure.

ACKNOWLEDGMENTS

We thank the Editor, Jeannot Trampert, Sjoerd de Ridder and an anonymous referee for their constructive comments. The reproducible numeric examples in this paper use the Madagascar open-source software package freely available from http://www.ahay.org.

REFERENCES

Araji, A., Revil, A., Jardani, A., Minsley, B. & Karaoulis, M., 2012. Imaging with cross-hole seismoelectric tomography hydrogeophysics, *Geophys. J. Int.*, **188,** 1285–1302.

Clærbout, J.F., 1985. *Imaging the Earth's Interior*, Blackwell Scientific Publications, Oxford.

De Ridder, S.A.L., Slob, E. & Wapenaar, K., 2009. Interferometric seismoelectric Green's function representations, *Geophys. J. Int.*, **178,** 1289–1304.

Fink, M., 1997. Time reversed acoustics, *Phys. Today*, **50,** 34–40.

Fink, M. & Prada, C., 2001. Acoustic time-reversal mirrors, *Inverse Probl.*, **17,** R1, doi:10.1088/0266-5611/17/1/201.

Frenkel, J., 1944. On the theory of seismic and seismoelectric phenomena in a moist soil, *J. Phys. (Soviet)*, **8,** 230–241.

Haines, S., 2004. Seismoelectric imaging of shallow targets, *PhD thesis*, Stanford University.

Helmholtz, H., 1879. Study concerning electrical boundary layers, *Weidemann Annal Physik Chemie*, **7,** 337–382.

Hu, H. & Liu, J., 2002. Simulation of the converted electric field during acoustoelectric logging, *Presented at the 72nd Annual International Meeting*, SEG, Expanded Abstracts.

Hu, H., Guam, W. & Harris, J., 2007. Theoretical simulation of electroacoustic borehole logging in a fluid-saturated porous formation, *J. acoust. Soc. Am.*, **122,** 135–145.

Jardani, A., Revil, A., Boleve, A., Dupont, J., Barrash, W. & Malama, B., 2007. Tomography of the Darcy velocity from self-potential measurements, *Geophys. Res. Lett.*, **34,** L24403, doi:10.1029/2007GL031907.

Jardani, A., Revil, A., Slobb, E. & Sollner, W., 2010. Stochastic joint inversion of 2D seismic and seismoelectric signals in linear poroelastic materials, *Geophysics*, **75,** N19–N31.

Parvulescu, A. & Clay, C., 1965. Reproducibility of signal transmissions in the ocean, *Radio Electron. Eng.*, **29,** 223–228.

Plessix, R.-E., 2006. A review of the adjoint state method for computing the gradient of a functional with geophysical applications, *Geophys. J. Int.*, **167,** 495–503.

Prada, C., Kerbrat, E., Cassereau, D. & Fink, M., 2002. Time reversal techniques in ultrasonic nondestructive testing of scattering media, *Inverse Probl.*, **18,** 1761–1773.

Pratt, R.G. & Worthington, M.H., 1990. Inverse theory applied to multisource cross-hole tomography. Part 1: acoustic wave-equation method, *Geophys. Prospect.*, **38,** 287–310.

Pride, S., 1994. Governing equations for the coupled electromagnetics and acoustics of porous media, *Phys. Rev. B*, **50**, 15 678–15 696.

Revil, A. & Jardani, A., 2010. Seismoelectric response of heavy oil reservoirs: theory and numerical modelling, *Geophys. J. Int.*, **180,** 781–797.

Rietbrock, A. & Scherbaum, F., 1994. Acoustic imaging of earthquake sources from the Chalfant valley 1986 aftershock series, *Geophys. J. Int.*, **119,** 260–268.

Schlumberger, C., 1920. *Etude sur la prospection lectrique du sous-sol (Study on Underground Electrical Prospecting)*, Gauthier-Villars et Cie, Paris.

Tarantola, A., 1984. Inversion of seismic reflection data in the acoustic approximation, *Geophysics*, **49,** 1259–1266.

Tarantola, A., 1987. *Inverse Problem Theory: Methods for Data Fitting and Model Parameter Estimation*, Elsevier, Amsterdam.

Thorbecke, J. & Wapenaar, K., 2007. On the relation between seismic interferometry and the migration resolution function, *Geophysics*, **72,** T61–T66.

Wang, M. & Revil, A., 2010. Electrochemical charge of silica surface at high ionic strength in narrow channels, *J. Colloid Interface Sci.*, **343,** 381–386.

Wenner, F., 1912. The four-terminal conductor and the Thomson Bridge, *U.S. Bur. Stand. Bull.*, **8,** 559–610.

Wenner, F., 1915. A method of measuring earth resistivity, *U.S. Bur. Stand. Bull.*, **12,** 469–478.

Woodward, M.J., 1992. Wave-equation tomography, *Geophysics*, **57,** 15–26.